

Pattern of flow around filter-feeding structures of immature *Simulium bivittatum* Malloch (Diptera: Simuliidae) and *Isonychia campestris* McDunnough (Ephemeroptera: Oligoneuriidae)

STEPHEN A. BRAIMAH¹

Department of Entomology, University of Alberta, Edmonton, Alta., Canada T6G 2E3

Received April 29, 1986

BRAIMAH, S. A. 1987. Pattern of flow around filter-feeding structures of immature *Simulium bivittatum* Malloch (Diptera: Simuliidae) and *Isonychia campestris* McDunnough (Ephemeroptera: Oligoneuriidae). *Can. J. Zool.* **65**: 514–521.

Filter feeding in immatures of *Simulium bivittatum* and *Isonychia campestris* is characterized by low Reynolds number (Re) (i.e., Re = 0.02–3.9). Scaled-up models of portions of filters towed through Canola oil revealed that capture of small particles occurs in the viscous boundary layer closest to the ray. Adhesion of such particles is enhanced by the reduction of velocity in the viscous layer with consequent increase in time for transit of particles in the filters. There was very little flow between adjacent rays of filters of larvae of *S. bivittatum* up to Re value of 0.49 (real life equivalent of 10.0 cm/s) and Re of 1.39 (17.5 cm/s) for nymphs of *I. campestris* because of boundary layer thickness. Microtrichia of *S. bivittatum* functioned as a virtually solid wall with no flow between adjacent microtrichia up to Re of 3.98 (80.0 cm/s) and for *I. campestris* up to Re of 7.79 (100.0 cm/s).

BRAIMAH, S. A. 1987. Pattern of flow around filter-feeding structures of immature *Simulium bivittatum* Malloch (Diptera: Simuliidae) and *Isonychia campestris* McDunnough (Ephemeroptera: Oligoneuriidae). *Can. J. Zool.* **65**: 514–521.

L'alimentation par filtration chez les larves de *Simulium bivittatum* et d'*Isonychia campestris* est caractérisée par des nombres de Reynolds (Re) faibles (i.e., Re = 0,02–3,9). Des modèles à l'échelle de portions de filtres ont été passés dans l'huile de Canola et l'expérience a démontré que la capture des particules fines se fait dans la couche visqueuse limitrophe qui se trouve le plus près du rayon. L'adhérence de ces particules est favorisée par la réduction de la vitesse dans la couche visqueuse, ce qui augmente la durée du passage des particules dans les filtres. Il y a très peu de courant entre les rayons adjacents des filtres chez les larves de *S. bivittatum* jusqu'à une valeur de Re de 0,49 (équivalent réel de 10,0 cm/s) et chez les larves d'*I. campestris* jusqu'à une valeur de Re de 1,39 (17,5 cm/s) à cause de l'épaisseur de la couche limitrophe. Les microtriches fonctionnent en fait à la manière d'un mur puisqu'il n'y a pas de courant entre les microtriches adjacentes jusqu'à une valeur de Re de 3,98 (80,0 cm/s) chez *S. bivittatum* et jusqu'à une valeur de Re de 7,79 (100,0 cm/s) chez *I. campestris*.

[Traduit par la revue]

Introduction

Suspension-feeding insects in freshwater environments have filters on specific parts of the body for capturing suspended particles. Exceptions to this are larvae that build nets. The filters of suspension-feeding black fly larvae consist of a pair of labral fans located on the head (Fig. 1). Mayfly species that feed on suspended materials have filters on their legs (Figs. 2 and 3). The function of filters as mechanical sieves has been well documented among the various groups of freshwater suspension-feeding insects. In addition to sieving, Braimah (1987) demonstrated the importance and applicability of direct interception, inertial impaction, gravitational deposition, and diffusion or motile-particle deposition to particle capture in suspension-feeding insects in freshwater environments.

When suspended particles reach a filter's surface by one or more of the four mechanisms they must be separated from the medium in which they are carried. Whether a particle is retained (captured) or not depends upon a number of factors.

The attachment efficiency, E_a , is a function of surface properties of filters and particles, and resident time of particles near filters. The latter factor is governed by the flow regime (whether it is laminar or turbulent) and the kinds of forces (inertial or viscous) that dominate flow.

A review of suspension feeding in flagellates, ciliates, sponges, copepods, bivalves, and ascidians (Jørgensen 1983) and other studies (O'Neil 1978; Koehl and Strickler 1981; Vogel 1981; Gerritsen and Porter 1982; Porter et al. 1983; LaBarbera 1984) showed that viscous forces play a more important role in particle capture in aquatic invertebrates than was previously realized. Earlier attempts to analyse particle

retention in passive, suspension-feeding, freshwater insects have given little attention to forces of fluid mechanical origin near filters. This lack of information of flow pattern was mostly due to difficulties involved in flow visualization because of the small size of filters. A more complete evaluation of particle capture by filter-feeding structures requires the use of scaled-up models to determine the actual pattern of flow around filters.

Scaled-up models facilitate flow visualization and make it easier to study fluid mechanical principles. If the Reynolds numbers for two systems are the same, then there is similarity in the streamline patterns in the model and prototype, and both have an equal drag coefficient, i.e., dynamic similarity (Fung 1969). Gerritsen and Porter (1982) used a scaled-up model made with 110- μm mesh plankton netting oscillated in glycerin to study boundary layer thickness at filtering setules on the appendage of *Daphnia magna* Straus. Silvester (1983) used nylon thread to study pressure drop across trichopteran filter nets by calculating changes in velocity of water flow through them. Scaled-up models of larvae of *Simulium vitattum* Zett. were used by Chance and Craig (1986) to demonstrate that aggregation is beneficial to feeding in this species of black fly. Wu et al. (1975) and Vogel (1981) are good sources for biological investigations that used scaled-up models.

The objective of this study was to use scaled-up models for flow visualization around filters of two suspension-feeding freshwater insects and to study the fluid mechanical principles exploited in separating particles from suspension.

Hydrodynamic principles that are relevant to suspension-feeding insects are outlined below.

Regimes of flow

In moving fluids, two types of flow, laminar or turbulent, may occur. Flow is laminar in situations where layers of fluid

¹Present address: 2541–116 Street, Edmonton, Alta., Canada T6J 3Z7.

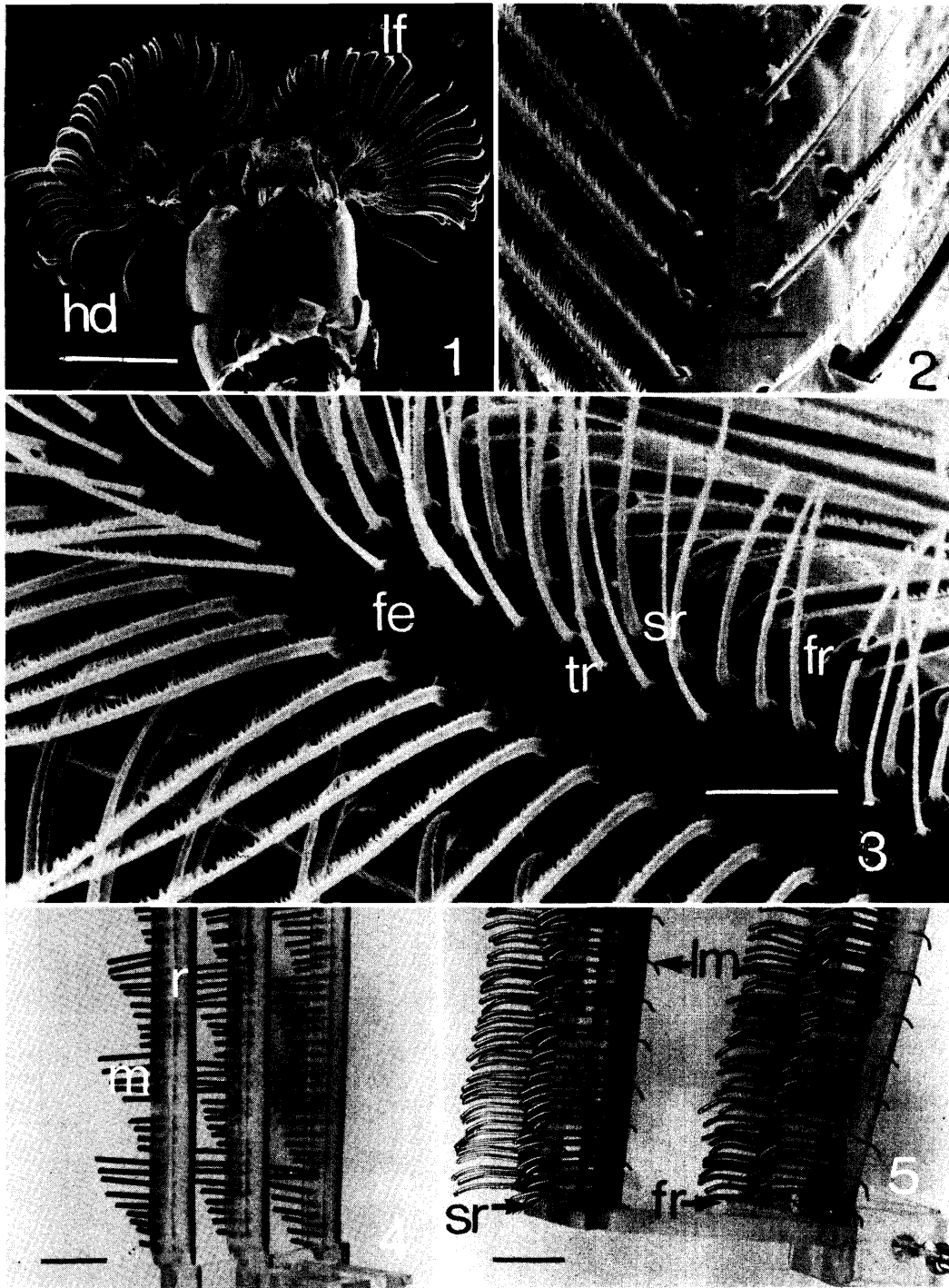


FIG. 1. Labral fans of *S. bivittatum*. Scale bar = 250 μm . FIG. 2. First and second rows of rays of foretibia of *I. campestris*. Scale bar = 25 μm . FIG. 3. First, second, and third rows of rays on forefemur of *I. campestris*. Scale bar = 40 μm . FIG. 4. Scaled-up model of portion of three rays of *S. bivittatum*. Scale bar = 2 cm. FIG. 5. Scaled-up model of portion of two rays on first and second rows of rays on foretibia of *I. campestris*. Scale bar = 2 cm. *fe*, femur; *fr*, first row; *hd*, head; *lf*, labral fans; *lm*, lateral microtrichia; *m*, microtrichia; *r*, ray; *sr*, second row; *ti*, tibia; *tr*, third row.

move downstream in smooth trajectories and all fluid particles move in parallel layers. In turbulent flow, the fluid particles move in an irregular manner though the mean direction of flow is downstream. The transition from laminar to turbulent flow occurs in a zone that is characterized by both types of flow.

Reynolds number

Reynolds number (Re) quantifies the relative importance of inertial (fluid momentum) forces and viscous (fluid stickiness) forces. Re indicates only the order of magnitude of the two

forces. The units of force cancel out, making Re a dimensionless number.

$$[1] \quad Re = UL\rho/\mu$$

where U = free stream velocity; L = characteristic length dimension; ρ = density of fluid medium; and μ = dynamic viscosity of medium. The ratio μ/ρ is called kinematic viscosity (ν).

In a given flow, different representatives of the characteristic

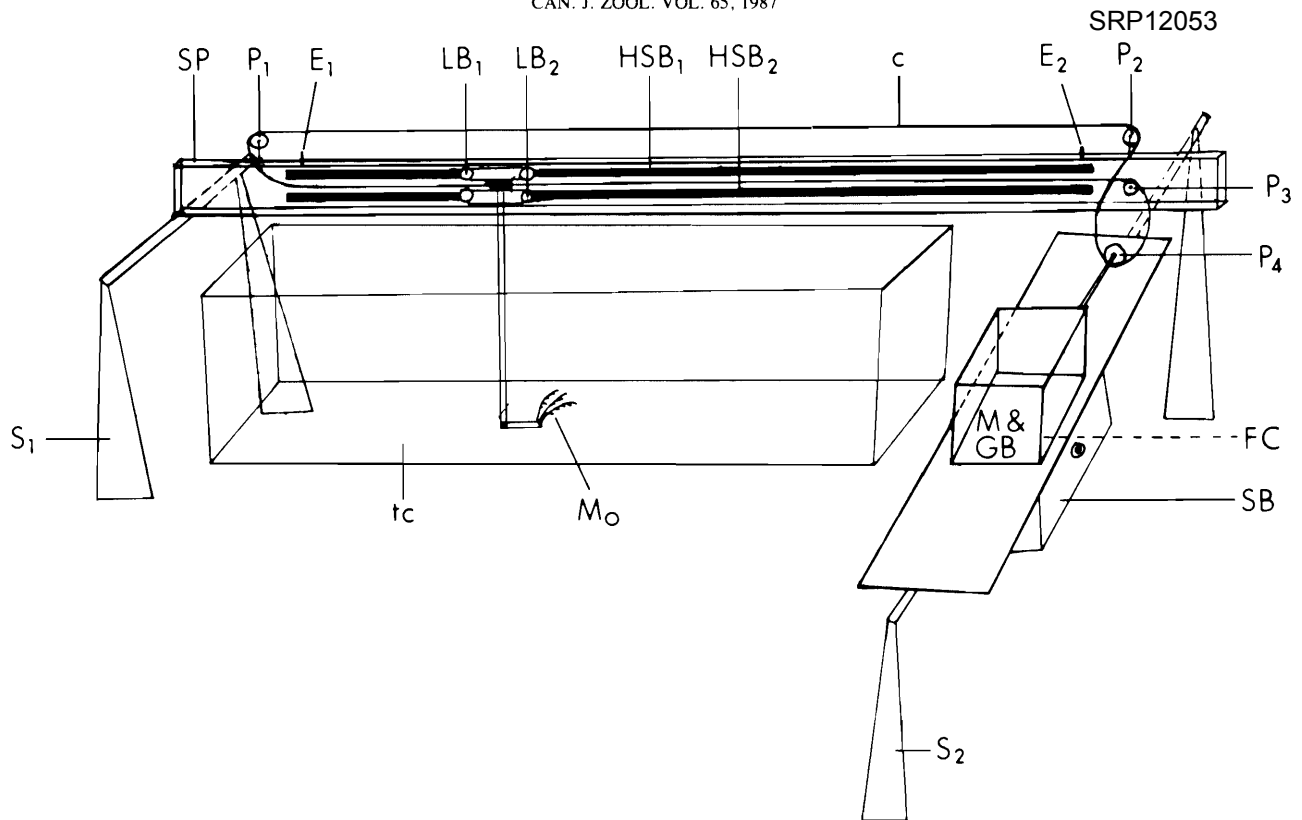


FIG. 6. Flow tank for towing scaled-up models of filter-feeding structures. *c*, towing cord; E_1 , E_2 , electrical start-stop contact; FC, feedback control to motor (M) and gear box (GB); HSB_1 , HSB_2 , hardened steel bar; LB_1 , LB_2 , linear bearing; M_o , model; P_1 , P_2 , P_3 , P_4 , pulleys; S_1 , S_2 , support; SB, switch box; SP, steel plate; *tc*, tank with Canola oil.

length dimension (L) may be chosen in defining Re , leading to different values for the number. In comparing flow systems with Re similarly defined, the system with the lower Re value has the more pronounced viscous effect.

Flow at Re less than 1 is characterized by large viscous forces, inertial forces being negligible (Fung 1969), and flow is typically laminar. Detailed fluid mechanics of flow dominated by viscous forces is given by Happel and Brenner (1965).

Velocity gradients and boundary layers

There is no slip (i.e., no relative motion) between a surface and the fluid layer immediately adjacent to it. This condition creates a velocity gradient near the surface due to subsequent layers of fluid slowing down. Velocity changes from zero at the surface to that of free stream flow some distance away. The thickness of the boundary layer (δ), or the regions of the fluid to which the viscous effect extends, is arbitrarily assumed to be the distance from the surface where the velocity has increased to at least 99% of the free stream flow (Schlichting 1960). Although, 99% is the most commonly used value, some authors (Streeter and Wylie 1979) use 90%. Vogel (1981) pointed out that the outer limit depends on the function for which one is invoking a boundary layer, and suggests that 90 probably has more biological significance.

Flow within a boundary layer may be laminar, transitional, or turbulent depending on the magnitude of the Re . At very low Re values the 90% boundary layer thickness δ is represented by

$$[2] \quad \delta = d/Re^{1/2} \text{ (Fung 1969)}$$

where d = diameter of object; Re = Reynolds number; and δ = thickness of boundary layer.

Drag in fluid flow

Drag is defined as the rate of removal of momentum from a moving fluid by an immersed body (Vogel 1981). The drag experienced by the body is represented by

$$[3] \quad \text{Drag} = \rho \int U_1 (U - U_1) \Delta S \text{ (Vogel 1981)}$$

where ρ = density of fluid at experimental temperature; U = free stream velocity; S = area of object exposed to flow; and U_1 = velocity at the downstream region (i.e., in the wake of the object).

Estimates of U_1 were based on velocity of particles in the region behind rays.

Materials and methods

Scanning electron micrographs of filters of simuliid larvae and ephemeropteran nymphs

Labral fans of simuliid larvae and forelegs of the ephemeropteran nymphs were prepared for SEM studies after the method of Ross and Craig (1979). Diameter and length of microtrichia, number of microtrichia per ray, number of rays per labral fan and per foreleg, and number of rows of rays per segment of foreleg were measured from photomicrographs.

Scaled-up models of portions of filters

Scaled-up models of portions of labral fans of larval *Simulium bivittatum* Malloch (Fig. 4) and rays on the forelegs of nymphs of *Isonychia campestris* McDunnough (Fig. 5) were made with Plexiglas and metal pins. Plexiglas and metal pins represent ray and microtrichia, respectively. The width and length of Plexiglas and metal pins were increased by a factor of 3000 over that of the actual insect structures. Relative shape, orientation, and dimension of each scaled-up model were determined from scanning electron micrographs.

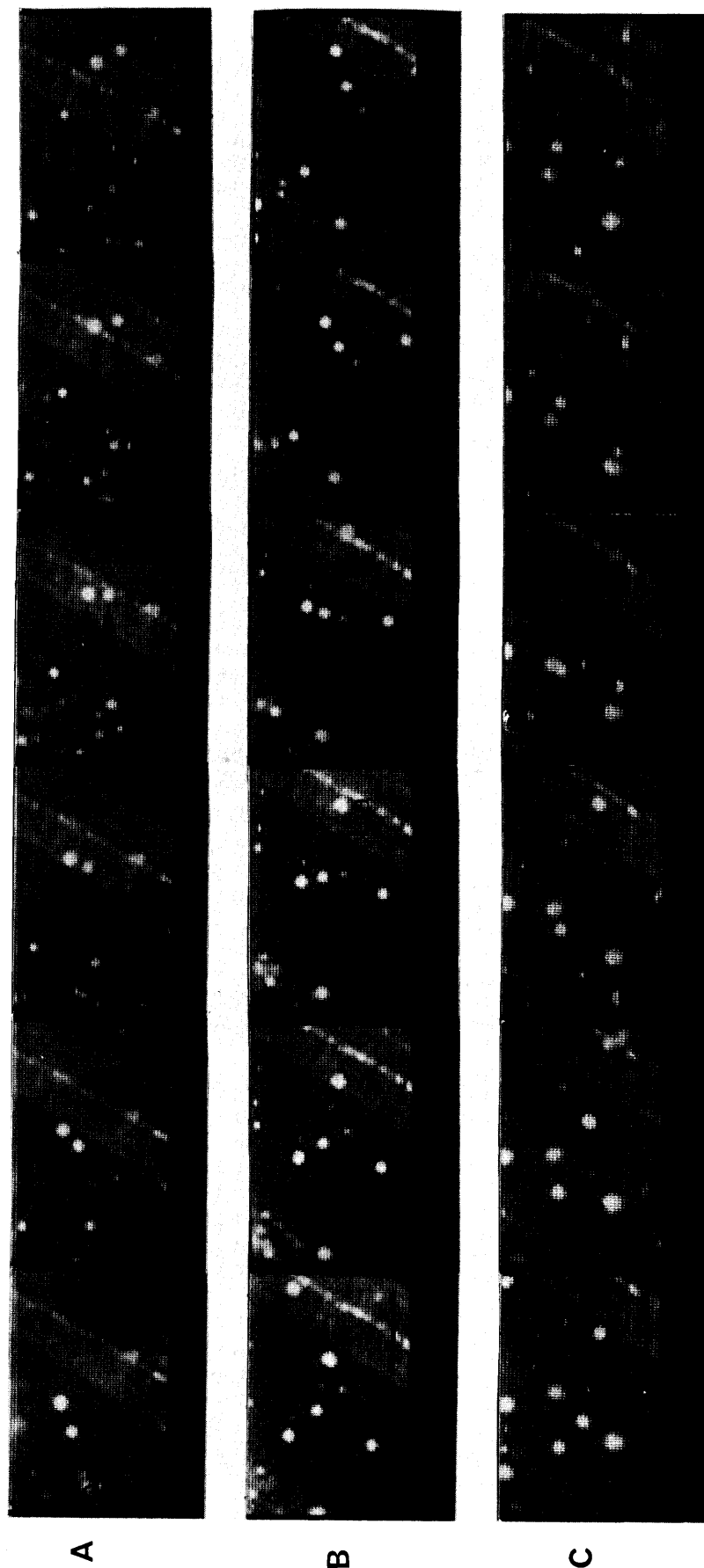


FIG 7. Sequence of photographs (from television monitor) of polystyrene particles in the boundary layer around scaled-up model of filter feeding structure of *Simulium bivittatum* Malloch. Arrows indicate direction of motion of particles in velocity gradients (see Table 1). Particles e and h in Fig. 7C have adhered to the filter and travelled with it in successive frames. Scale bar = 1 cm.

TABLE 1. Velocity of polystyrene particles in velocity gradients in the boundary layer around scaled-up model of labral fan of immature *S. bivittatum* Malloch

Distance from filter (cm)	Velocity (cm/s)	Figure
0	0	7C, e
0	0	7C, h
0.40	5.4×10^{-2}	7A, b
0.70	9.1×10^{-2}	7A, a
0.61	7.2×10^{-2}	7B, d
0.85	10.0×10^{-2}	7B, c
1.03	12.6×10^{-2}	7C, f
1.28	15.3×10^{-2}	7C, g

The area of the model of labral fans of simuliid larva was calculated using the following equation:

$$[4] \quad \Delta S = R \times (A + (I \times M)) \text{ (Ross and Craig 1980)}$$

$$[5] \quad I = \pi r(r^2 + h^2)^{1/2}$$

where r = average radius of microtrichia; h = average height of microtrichia; I = average surface area of a microtrichia; R = average number of rays per labral fan or foreleg; M = average number of microtrichia per ray; and A = average surface area of both sides of a labral fan ray.

Area of rays on each row of the forelegs of nymphs of *I. campestris* was calculated using the following formula:

$$[6] \quad \Delta S = R \times (A + (I \times M_1) + (I \times M_2))$$

where M_1 = average number of microtrichia for first row of rays; and M_2 = average number of microtrichia for second row of rays.

Towing experiments

The models were towed through Canola oil at various velocities by a gear-reduced type NSH-12 Fractional Horsepower motor (Bodine Electric Co., Chicago, Illinois) attached to a model SL 15 Minarik feedback control (Minarik Electric Co., Los Angeles, California). A trolley to which the models were attached was mounted on two linear bearings and pulled (Fig. 6). This arrangement reduced vibration to the models and improved flow visualization. Electrically controlled start-stop contacts were used to maintain a fixed distance of 68.0 cm travelled by each model. The oil was cooled to 10°C to achieve the desired dynamic viscosity of 143.0 cP. Two size classes (≈ 2.0 and ≈ 4.0 μm) of polystyrene particles, to represent 0.5 and 1.2 μm particles, respectively, were added to the oil. Particles were kept in suspension by stirring. An interval of 30 s was required between each experiment to allow the turbulence created by stirring to subside. Reynolds number (Re), boundary layer thickness (δ), and drag were calculated for each model at various velocities. These values were compared with those for live immatures of both insects by invoking the principle of dynamic similarity (Fung 1969; Francis 1975; Vogel 1981; Koehl and Strickler 1981). Observations were recorded by a Panasonic video camera with a Micro-Nikkor 105-mm lens. Frame by frame analysis of the tape was made with Sony Automatic Editing Unit, RM-440.

Boundary layer around models

Photographs of polystyrene particles in different velocity gradients (Fig. 7) in the laminar boundary layer around each ray were taken from the video monitor. The editing unit was switched to manual mode so that frame by frame analysis could be done. Two fields of interlacing scan lines make up one television frame (i.e., one field = 1/60 s). Photographs were taken with a Canon A1 camera with an 80- to 210-mm macro zoom lens, and a 2 \times Tameron convertor Tri-X film rated at ISO 800 was used. Exposure was 1/8 s at F4.

TABLE 2. Calculated drag for filtering structures of live immatures of *I. campestris* McDunnough and *S. bivittatum* Malloch

	Range of velocity (cm/sc)		Drag (N)
	U	U_1	
<i>I. campestris</i>	0.80–0.90	0.40–0.45	9.20×10^{-5}
	6.00–6.20	4.00–4.65	380.10×10^{-5}
<i>S. bivittatum</i>	0.80–0.85	0.30–0.35	3.50×10^{-5}
	6.00–6.20	5.00–6.00	22.0×10^{-5}

NOTE: U , free stream velocity; U_1 , velocity at the downstream region.

Velocity gradients in boundary layer around filters

The distance of polystyrene particles from the surface of rays and microtrichia (Table 1) was approximated using the following equation:

$$[7] \quad \delta U_x / \delta y = 0.32 U^{3/2} \rho_c^{1/2} X^{-1/2} \mu_c^{-1/2} \text{ (Vogel 1981)}$$

where $\delta U_x / \delta y$ = rate of change in velocity along microtrichia and ray; X = distance downstream from leading edge of microtrichia and associated ray; U = free stream velocity; ρ_c = density of Canola oil; μ_c = dynamic viscosity of Canola oil.

Calculations and results

Drag

Results indicate that drag on the filters of nymphs of *I. campestris* was greater than on the filters of *S. bivittatum* at all current velocities (Table 2). Immatures of *I. campestris* have a higher relative increase in drag on filters from low to high velocities. There was a 6-fold increase for larvae of *S. bivittatum* and a 40-fold increase for larvae of *I. campestris* (Table 2).

Reynolds number (Re)

Particle capture by microtrichia and rays of both insects (Tables 3 and 4) occurs at low Re values of 0.02–3.2. The lowest Re for the models was less than the lowest Re for live insects, but a higher Re was obtained with models. The range of overlap of Re values was large enough to enable comparison of flow patterns between models and live insects at Re values of 0.07–2.11 for larvae of *S. bivittatum* and Re values of 0.07–3.24 for nymphs of *I. campestris*.

Boundary layer (δ)

Boundary layer thickness around each microtrichium of live larvae of *S. bivittatum*, even at maximum velocity of 47.0 cm/s, extended to the fifth microtrichium away from it. Models indicate that boundary layer thickness around each microtrichium extended to the next microtrichium at Re value of 3.98 (80.2 cm/s). Boundary layer thickness around each microtrichium in the first row of models of rays of *I. campestris* nymphs extended to the third microtrichium at maximum Re of 7.97 (100.0 cm/s). Thus, there was virtually no flow between individual microtrichia. Distance between adjacent rays and thickness of boundary layer around each ray indicate that there was very little flow between rays up to Re values of 0.49 for larvae of *S. bivittatum* and up to Re values of 1.39 for rays on the first row of filters of nymphs of *I. campestris*.

Pattern of flow around models

Flow pattern at $Re < 1$ (real life equivalent of 20.0 cm/s)

Simulium bivittatum—Generally, there was very little flow between adjacent rays. Flow was dominated by viscous forces and concomitant reversal of flow. Polystyrene particles travelled with the models in the deep boundary layer that surrounded

TABLE 3. Some calculated values of velocity, Reynolds number (Re), and boundary layer thickness for live larvae and scaled-up model of portion of labral fan of *S. bivittatum* Malloch

Velocity (cm/s)	N*	Reynolds number (Re)		Thickness of boundary layer†	
		Ray	Microtrichia	Ray	Microtrichia
Model					
0.54(0.02)‡	5	0.35(0.02)	0.07(0.004)	1.90(0.07)	0.76(0.02)
1.62(0.01)	3	1.04(0.01)	0.21(0.002)	1.10(0.02)	0.44(0.004)
4.00(0.01)	2	2.58(0.02)	0.52(0.002)	1.68(0.002)	0.28(0.001)
6.18(0.01)	2	3.98(0.01)	0.79(0.01)	1.55(0.002)	0.23(0.002)
Live larvae					
0.6(0.28)	3	0.17(0.01)	0.04(0.003)	12.12(0.49)	5.00(0.26)
9.8(0.58)	9	0.49(0.03)	0.10(0.006)	7.14(0.31)	3.16(0.13)
31.6(2.89)	14	1.57(0.14)	0.31(0.03)	3.99(0.25)	1.79(0.13)
42.6(2.82)	12	2.11(0.15)	0.42(0.03)	3.44(0.17)	1.54(0.07)

*Number of replicates.

†In cm for model, in μm for live larvae.

‡Mean, with SD in parentheses.

TABLE 4. Some calculated values of velocity, Reynolds number (Re), and boundary layer thickness for first row of filtering rays and for scaled-up model of rays of *I. campestris*

Velocity (cm/s)	N*	Reynolds number (Re)		Thickness of boundary layer†	
		Ray	Microtrichia	Ray	Microtrichia
Live nymphs					
3.4(0.14)‡	6	0.27(0.02)	0.02(0.001)	15.53(0.82)	4.73(0.17)
9.6(0.46)	7	0.77(0.05)	0.06(0.004)	9.19(0.42)	2.73(0.13)
30.2(1.9)	10	2.42(0.22)	0.20(0.02)	5.19(0.33)	1.50(0.11)
40.5(1.0)	7	3.24(0.11)	0.30(0.01)	4.48(0.11)	1.22(0.03)
Scaled-up model					
First row					
0.54(0.02)	5	0.70(0.04)	0.07(0.004)	2.15(0.09)	0.76(0.02)
0.85(0.01)	5	1.09(0.02)	0.11(0.002)	1.72(0.02)	0.60(0.008)
0.23(0.02)	3	6.75(0.04)	0.67(0.02)	0.69(0.002)	0.24(0.001)
0.18(0.01)	3	7.97(0.02)	0.79(0.01)	0.64(0.001)	0.23(0.002)
Second row					
0.00	5	0.00	0.00	Very thick	Very thick
0.00	5	0.00	0.00	Very thick	Very thick
2.86(0.04)	3	3.96(0.02)	0.37(0.01)	0.94(0.002)	0.33(0.01)
5.30(0.02)	3	6.84(0.04)	0.68(0.01)	0.69(0.02)	0.24(0.02)

*Number of replicates.

†In cm for model, in μm for live nymphs.

‡Mean, with SD in parentheses.

rays and microtrichia. Most of the large particles in the viscous layer sedimented. At the end of each towing run there were more smaller particles on the rays and microtrichia.

Isonychia campestris—Pattern of flow observed was similar to that of larvae of *S. bivittatum*. When there was very little flow between the first row of rays, particles that entered the boundary layer between the first and second rows of rays travelled in the same direction as the models. Larger particles in the zone sedimented. Rays in the first row captured more particles than rays in the second row. Size of particles captured by rays in both rows was similar to that observed for larvae of *S. bivittatum*.

Flow pattern at $1 < Re < 8$ (real life equivalent of 30.0–100.0 cm/s)

Simulium bivittatum ($1 < Re < 4$; real life equivalent of 30.0–80.0 cm/s)—The effect of viscous forces decreased

considerably at Re above 1.0, although it was still noticeable at Re up to 1.5. The boundary layer around each ray was thinner and there was flow between adjacent rays. Generally the velocity gradients around each ray and microtrichia steepened. Particles in faster gradients were observed to overtake particles in the slower gradients near rays and microtrichia (Fig. 7). The effect of viscous forces decreased even further around Re of 3 with consequent decrease in thickness of boundary layer and faster flow between adjacent rays. Sedimentation rate of large particles also decreased. The majority of particles captured were in the smaller size class even at the maximum Re of 4.0.

Isonychia campestris ($1 < Re < 8$; real life equivalent of 17.5–100.0 cm/s)—Pattern of flow observed for rays on the first row was similar to that of larvae of *S. bivittatum* except that viscous forces were more noticeable. There was flow between rays on the second row where Re was 0.7 (Table 4). The dead

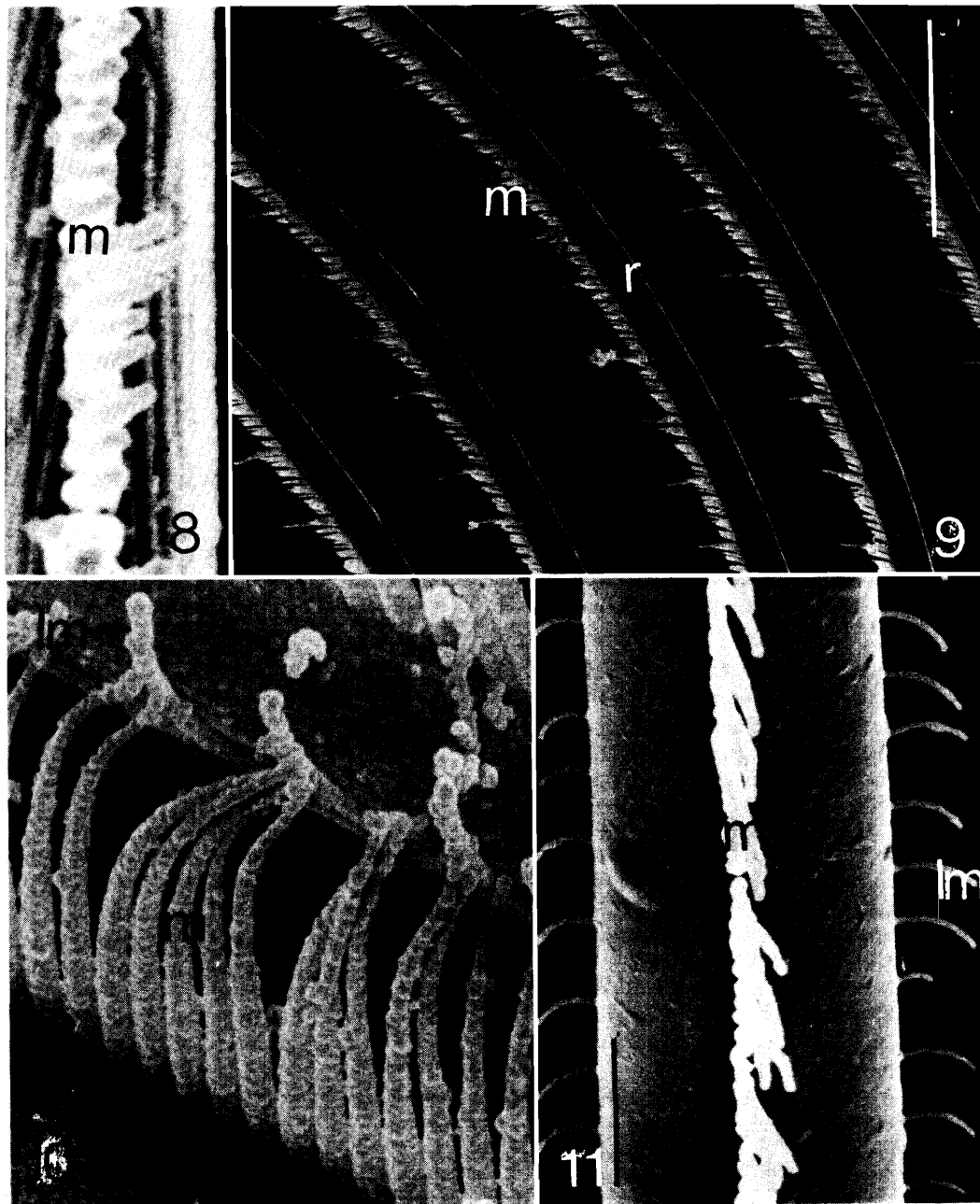


FIG. 8. Frontal view showing orientation of ray and microtrichia of *S. bivittatum* to flow. Scale bar = 2 μm . FIG. 9. Lateral view of rays of *S. bivittatum*. Scale bar = 25 μm . FIG. 10. Polystyrene particles caught by secretions on microtrichia and rays of filters of *I. campestris*. Scale bar = 2 μm . FIG. 11. Frontal view showing orientation of ray and microtrichia to flow in *I. campestris*. Scale bar = 4 μm . *lm*, lateral microtrichia; *m*, microtrichia; *po*, polystyrene particle; *r*, ray.

zone between the first and second row of rays became mobile at Re of 3.0, but sedimentation of large particles continued in the zone at a slower rate. There was considerable decrease in the effect of viscous forces in the zone at Re of 5.0, resulting in steeper velocity gradients and decreased sedimentation of larger particles. The number of smaller particles captured at higher Re values was less than at Re less than 1.0.

Discussion

Structure of filters and particle capture

Simulium bivittatum

Larvae capture suspended particles by presenting mucosubstance-coated microtrichia (Figs. 8 and 9) to currents. It has

been suggested by Ross and Craig (1980) that the mucosubstances may be negatively charged. It is also possible that these substances change the surface chemistry of microtrichia and rays to enhance particle attachment by hydrophobic-hydrophilic and ionic interaction (Gerritsen and Porter 1982). The thickness of the boundary layer (Tables 3 and 4) is such that there was virtually no flow between individual microtrichia, even at the maximum Re of 2.11 (real velocity equivalent of 42.0 cm/s). Parallel filter orientation and arrangement reduces drag (Spielman 1977; Vogel 1981), but it also reduces capture efficiency because of the small surface area exposed to flow.

Isonychia campestris

The double row of rays on the tibia and tarsus (Fig. 2) and

triple row on the part of the femur closer to the trochanter (Fig. 3) create a zone of little or no flow in the area immediately in front of the second and third rows of microtrichia, because of overlap of boundary layers. Scaled-up models of portions of the filters show that this zone of overlap exists up to Re of about 3.0. Parallel orientation of filters to flow (Figs. 10 and 11) reduces drag but the number and arrangement of filters also increases the amount of surface exposed to flow with a consequent increase in drag; this may restrict nymphs to slower currents. The second and third rows of microtrichia are operating at highly reduced Re compared with rays in the first row.

Although no mucosubstance-secreting organ is known from mayflies, observations from this study (Fig. 10) show that nymphs of *I. campestris* can capture suspended particles from suspension. A possible cause of adhesion may be hydrophobic-hydrophilic or ionic interaction between particles and filters (Gerritsen and Porter 1982). The latching of microtrichia to lateral microtrichia (Fig. 10) increases the probability of particle capture. Particles in the slowest velocity gradient, that of the viscous boundary layer closest to the ray, must pass by two and sometimes three or four rays latched together in a plane parallel to flow. The consequent increase in time for transit of particles past latched rays enhanced particle capture. Latching occurs mostly at the distal end of some rays but most rays functioned as isolated cylindrical collectors.

Generally, adhesion of particles to filters, in both insects, occurs in the slowest velocity gradient of the viscous boundary layer (Fig. 7C, *h* and *e*). The geometry and dimensions of filter-feeding structures used in this study and observations of filters of other suspension feeders (author's unpublished data), together with velocities encountered in nature and basic hydrodynamics, indicate that laminar flow (low Re) is a generality among passive suspension-feeding animals. A suggestion similar to this was made by Vogel (1981), who also indicated that the only high Re suspension feeder may be the baleen whale.

Acknowledgements

I thank J. S. Scott for assistance with figures, M. McIntyre for help in building flow tanks, and G. Braybrook for assistance with the scanning electron microscope. I am grateful to Vera Braimah for help in field and laboratory experiments. Reviews and advice from M. LaBarbera and D. A. Craig helped in preparation of the manuscript. Financial support was provided from Natural Sciences and Engineering Research Council of Canada grant No. A-5753 to D. A. Craig.

- BRAIMAH, S. A. 1987. Mechanisms of filter feeding in immature *Simulium vibittatum* Malloch (Diptera: Simuliidae) and *Isonychia campestris* McDunnough (Ephemeroptera: Oligoneuriidae). *Can. J. Zool.* **65**. This issue.
- CHANCE, M. M., and D. A. CRAIG. 1986. Hydrodynamics and behaviour of Simuliidae larvae (Diptera). *Can. J. Zool.* **64**: 1295–1309.
- FRANCIS, J. R. D. 1975. Fluid mechanics. William Clowes and Sons Ltd., London.
- FUNG, Y. C. 1969. A first course in continuum mechanics. Prentice-Hall, Inc., Englewood Cliffs, NJ.
- GERRITSEN, J., and K. G. PORTER. 1982. The role of surface chemistry in filter feeding by zooplankton. *Science* (Washington, D.C.), **216**: 1225–1227.
- HAPPEL, J. L., and H. BRENNER. 1965. Low Reynolds number hydrodynamics. Prentice-Hall, Inc., Englewood Cliffs, NJ.
- JØRGENSEN, C. B. 1983. Fluid mechanical aspects of suspension feeding. *Mar. Ecol. Prog. Ser.* **11**: 89–103.
- KOEHL, M. A. R., and J. R. STRICKLER. 1981. Copepod feeding currents: food capture at low Reynolds number. *Limnol. Oceanogr.* **26**: 1062–1073.
- LABARBERA, M. 1984. Feeding currents and particle capture mechanisms in suspension-feeding animals. *Am. Zool.* **24**: 71–84.
- O'NEIL, P. L. 1978. Hydrodynamic analysis of feeding in sand dollars. *Oecologia*, **34**: 157–174.
- PORTER, K. G., Y. S. FEIG, and F. F. VETTER. 1983. Morphology, flow regimes, and filtering rates of *Daphnia*, *Ceriodaphnia* and *Bosmina* fed natural bacteria. *Oecologia*, **58**: 156–163.
- ROSS, D. H., and D. A. CRAIG. 1979. The seven larval instars of *Prosimulium mixtum* Syme and Davies and *P. fuscum* Syme and Davies (Diptera: Simuliidae). *Can. J. Zool.* **57**: 290–300.
- . 1980. Mechanisms of fine particle capture by larval black flies (Diptera: Simuliidae). *Can. J. Zool.* **58**: 1186–1192.
- SCHLICHTING, H. 1960. Boundary layer theory. McGraw-Hill Book Co., New York.
- SILVESTER, N. R. 1983. Some hydrodynamic aspects of filter feeding with rectangular-mesh nets. *J. Theor. Biol.* **103**: 265–286.
- SPIELMAN, L. A. 1977. Particle capture from low-speed laminar flows. *Annu. Rev. Fluid Mech.* **9**: 297–319.
- STREETER, V. L., and E. B. WYLIE. 1979. Fluid mechanics. McGraw-Hill Book Co., New York, Montreal, Ackland, and Toronto.
- VOGEL, S. 1981. Life in moving fluids: the physical biology of flow. Willard Grant Press, Boston, MA.
- WU, T.Y.-T., C. J. BROKAW, and C. BRENNEN (Editors). 1975. Swimming and flying in nature. Plenum Press, New York.